Synthesis and Reactivity of Iron Complexes with a New Pyrazine-Based Pincer Ligand, and Application in Catalytic Low-Pressure Hydrogenation of Carbon Dioxide

Orestes Rivada-Wheelaghan,[†] Alexander Dauth,[†] Gregory Leitus,[‡] Yael Diskin-Posner,[‡] and David Milstein*,[†]

[†]Department of Organic Chemistry and [‡]Department of Chemical Research Support, Weizmann Institute of Science, Rehovot 76100, Israel

S *Supporting Information*

ABSTRACT: A novel pincer ligand based on the pyrazine backbone (PNzP) has been synthesized, (2,6-bis(di(*tert*-butyl)-phosphinomethyl)pyrazine), tBu-PNzP. It reacts with $FeBr_2$ to yield $[Fe(Br)_2(tBu\text{-}PNzP)]$, **1**. Treatment of **1** with $NaBH_4$ in MeCN/MeOH gives the hydride complex $[Fe(H)-(MeCN)_2(tBu\text{-}PNzP)][X]$ (X = Br, BH_4), **2·X**. Counterion exchange and exposure to CO atmosphere yields the complex *cis*-$[Fe(H)(CO)(MeCN)(tBu\text{-}PNzP)][BPh_4]$ **4·BPh$_4$**, which upon addition of Bu_4NCl forms $[Fe(H)(Cl)(CO)(tBu\text{-}PNzP)]$ **5**. Complex **5**, under basic conditions, catalyzes the hydrogenation of CO_2 to formate salts at low H_2 pressure. Treatment of complex **5** with a base leads to aggregates, presumably of dearomatized species **B**, stabilized by bridging to another metal center by coordination of the nitrogen at the backbone of the pyrazine pincer ligand. Upon dissolution of compound **B** in EtOH the crystallographically characterized complex **7** is formed, comprised of six iron units forming a 6-membered ring. The dearomatized species can activate CO_2 and H_2 by metal−ligand cooperation (MLC), leading to complex **8**, *trans*-[Fe(PNzPtBu-COO)(H)(CO)], and complex **9**, *trans*-[Fe(H)$_2$(CO)(tBu-PNzP)], respectively. Our results point at a very likely mechanism for CO_2 hydrogenation involving MLC.
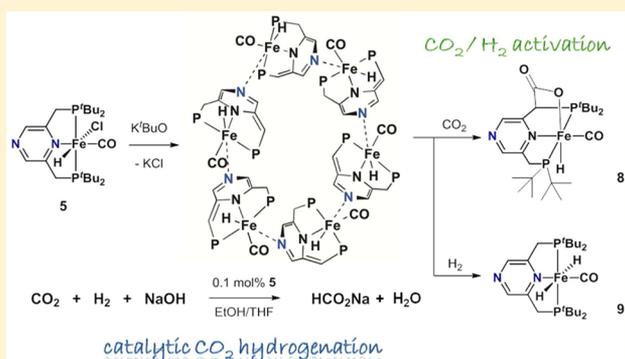
INTRODUCTION

In recent years there has been much interest in catalysis by iron complexes due to their abundance, low toxicity, and low price and the benign environmental impact of iron compounds.[1] In particular, iron pincer complexes have gained interest as catalysts. Brookhart and Gibson independently reported in 1998 the application of bis(imino)pyridine iron complexes as catalysts in olefin oligomerization and polymerization reactions.[2] Chirik and co-workers have shown the excellent catalytic properties of these bis(imino)pyridine−iron complexes for hydrosilylation and hydrogenation of alkenes and alkynes and also their activity in C−C bond formation.[3] An interesting feature of this ligand is the noninnocent behavior of the imine groups attached to the metal center, which are able to delocalize electrons from the metal center.[4] Several other iron−pincer complexes have been developed recently, some showing catalytic activity in amino−borane dehydrogenation or improving alkene hydrosilylation reactions.[5] The *trans*-[FeH-(BH$_4$)(CO)(iPr-PN(H)P)] complex, reported by Hazari, Schneider, and Beller,[6] exhibits high catalytic activity in hydrogenation and dehydrogenation processes.[7] Our group has developed Fe−PNP and Fe−PNN pincer complexes based on N-heterocyclic aromatic rings (Figure 1).[8] An important
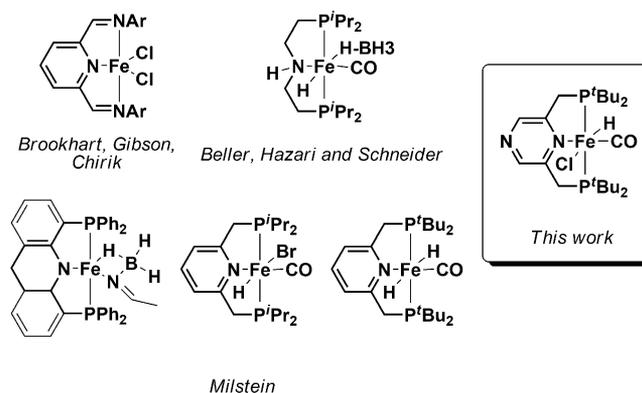
Figure 1. Selection of iron pincer complexes used in catalysis.

feature of the lutidine-based ligands is the ease of deprotonation of the benzylic CH$_2$ group, resulting in dearomatization. As we have shown, metal−ligand cooperation (MLC) involving the metal center and the dearomatized pincer ligand can result in the activation of various X−H bonds (X =

H, C, O, N, B).[9] We now report a novel pincer ligand based on a pyrazine backbone (PNzP). While this PNzP ligand keeps the possibilities open for MLC by aromatization/dearomatization of the pyrazine ring, the nitrogen atom in position 4 of the heterocycle expands its scope of reactivity as compared to our earlier studies on pyridine-based PNP ligand systems.[9] In principle, the electronic properties of the ligand and metal can be tuned by complexation to the nitrogen in position 4. A recent example showing such a behavior was observed by Bergman, Tilley, and co-workers,[10] in which biaryl reductive elimination was accelerated in a system based on a bipyrazine–diarylplatinum(II) complex by Lewis acid binding at the nitrogen atom in position 4. Moreover, the N atom can stabilize intermediates by intermolecular coordination. Several years ago, we reported PCP-type complexes based on lutidine, in which the nitrogen atom resides at position 4 and is available for further reactivity.[11]

Iron complexes developed by our group are excellent catalysts for the hydrogenation of various substrates.[8b−e,h] In this report we present the synthesis of a series of iron complexes bearing the new PNzP ligand, with one of them used successfully for catalytic hydrogenation of CO_2 to a formate salt under low pressure and mild conditions. The use of carbon dioxide as a C1 source for chemical transformations[12] is an important research field, including transformation of CO_2 into formates.[13] We demonstrated the active participation of the PNzP ligand in H_2 and CO_2 activation by MLC and characterized several possible intermediates involved in the catalytic hydrogenation of CO_2, including characterization by X-ray diffraction of a catalytic species, a metallomacrocycle composed by 6 iron−PNzP units being bridged by the N atom in position 4.

RESULTS AND DISCUSSION

Ligand Synthesis and Complexation with Iron. The new ^{t}Bu-PNzP (2,6-bis(di-*tert*-butylphosphinomethyl)pyrazine) ligand was synthesized in two steps starting with 2,6-dimethylpyrazine. In the first step, chlorination of the methyl groups to yield 2,6-bis(chloromethyl)pyrazine was achieved by a radical reaction with *N*-chlorosuccinimide using the protocol of Neugebauer.[14] In the second step, the chlorides were substituted by di(*tert*-butyl)phosphine following a method previously used in our group to give the tBu-PNzP ligand in good yields (Scheme 1).[15] The $^{31}P\{^1H\}$ NMR spectrum of the new ligand exhibits a singlet at $\delta = 39.4$ ppm, similar to the tBu-PNP ligand[15] (tBu-PNP denotes the ligand based on the pyridine backbone).

The reaction of tBu-PNzP with 1 equiv of $FeBr_2$ in THF yielded the paramagnetic complex $[Fe(Br)_2(tBu-PNzP)]$, **1** (Scheme 1). The solution magnetic moment of **1** ($\mu_{eff} = 5.57$),

Scheme 1. Ligand Synthesis and Complexation with Iron[a]
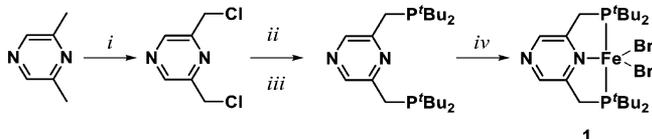
[a]Conditions: (i) *N*-Chlorosuccinimide (NCS) (2.5 equiv), benzoyl peroxide (0.02 equiv), in CCl_4, reflux, 12 h.(ii) HP^tBu_2 (3 equiv), in MeOH, 60° C, 48 h. (iii) Addition of 4 equiv of Et_3N and work up. (iv) $FeBr_2$ (0.95 equiv) in THF, 12 h.

measured by Evan's method,[16] fits well for an Fe(II) d[6] with high-spin configuration.[8f] Crystals of **1** suitable for X-ray diffraction were obtained by slow diffusion of pentane into a concentrated THF solution (Figure 1). The solid state structure of complex **1** (Figure 2) is best described as a
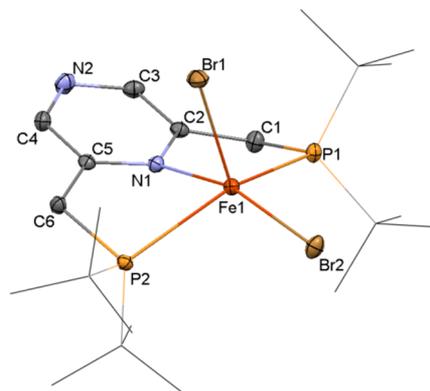
Figure 2. X-ray structure of complex **1**; thermal ellipsoids set at 50% probability level, and the *tert*-butyl groups are presented as wireframe for clarity. Selected bond lengths (Angstroms) and angles (degrees): Fe1−Br1 2.442(1), Fe1−Br2 2.491(1), Fe1−P1 2.527(1), Fe1−P2 2.506(1), Fe1−N1 2.352(2), N1−C2 1.346(2), N1−C5 1.341(2), N2−C3 1.337(2), N2−C4 1.331(2), C2−C3 1.378(2), C4−C5 1.377(2), P1−Fe1−P2 138.01(1), Br1−Fe1−Br2 105.01(1), N1−Fe1−Br2 101.01(3), N1−Fe1−Br1 93.05(3), P1−Fe1−N1 75.56(4), P2−Fe1−N1 73.69(4).

distorted square pyramid with a τ value of 0.39,[17] in which the angles are in the range 73.69(4)−138.01(1)°, the iron atom lying 0.540 Å out of the basal plane (defined by P1, N1, Br2, P2) in the direction of the apical Br1 atom. The bond distance of Fe1−P2 (2.506(1) Å) is slightly shorter than that of Fe1−P1 (2.527(1) Å); interestingly the Fe1−N1 bond length (2.352(2) Å) is significantly longer than that found for the similar iron dichloride complex bearing the tBu-PNP ligand (Fe−N, 2.198(4) Å).[18] The Fe1−Br1 (axial) distance (2.442(1) Å) is shorter than its basal counterpart.

Synthesis of (tBu-PNzP)Fe Hydride Complexes. Previous studies showed that addition of $NaBH_4$ in MeCN/EtOH to a mixture of tBu-PNP ligand and $FeBr_2$ followed by treatment with 1 bar of CO yielded the dihydride complex $[Fe(H)_2(CO)(tBu-PNP)]$, which is an excellent catalyst for the hydrogenation of CO_2 to formate salt.[8c] An analogous procedure using the new tBu-PNzP ligand resulted in decomposition. In addition, complex **1** does not bind CO; hence, we were unable to prepare a Fe(H)CO complex by this route, unlike the reported procedures in the literature.[6a,b,8b] On the other hand, reaction of **1** with 2.2 equiv of $NaBH_4$ in a mixture of MeOH/MeCN gave a deep blue solution containing a complex that is tentatively identified as a mixture of complexes **2·X**, $[Fe(H)(MeCN)_2(tBu-PNzP)][X]$ (X = Br or BH_4), according to the NMR data (Scheme 2). The new blue compound exhibits in the ^1H NMR spectrum in CD_3CN a triplet signal at $\delta = -12.31$ ppm for the hydride ligand. Two multiplets at $\delta = 3.22$ and 3.41 ppm (2H each) that are assigned to the benzylic methylene groups of the pincer ligand are indicative of a nonsymmetric pattern across the plane of the heterocycle suggesting a cis arrangement. The phosphorus atoms resonate at 107 ppm in the $^{31}P\{^1H\}$ NMR spectrum. Unfortunately the instability of this complex in solution (except in acetonitrile) precluded its full characterization. Nevertheless,

Scheme 2. Formation of Complex 2·BPh₄, and Postulated Oligomerization in the Solid State

i : 2.2 eq. NaBH₄ , MeCN / MeOH

ii : 1 eq. NaBPh₄ , MeCN
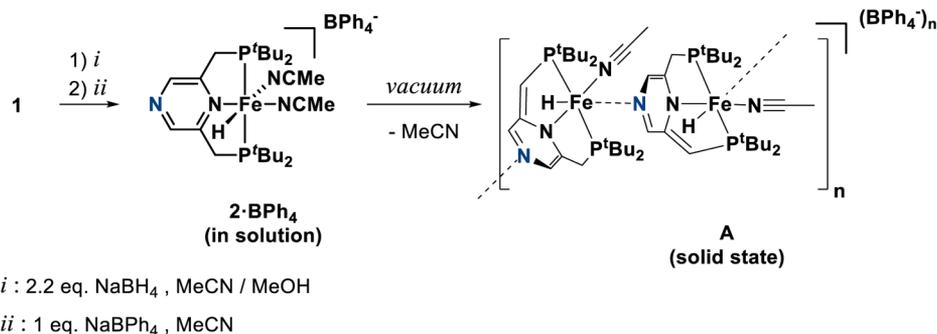
Scheme 3. (tBu-PNzP)Fe Hydride Complexes

i : 2.2 eq. NaBH₄ , MeCN / MeOH
ii : 1 eq. NaBPh₄
iii : 1bar CO / MeCN
iv : 90ºC , 30 min / MeCN
v : 2.2 eq. Bu₄NCl / THF
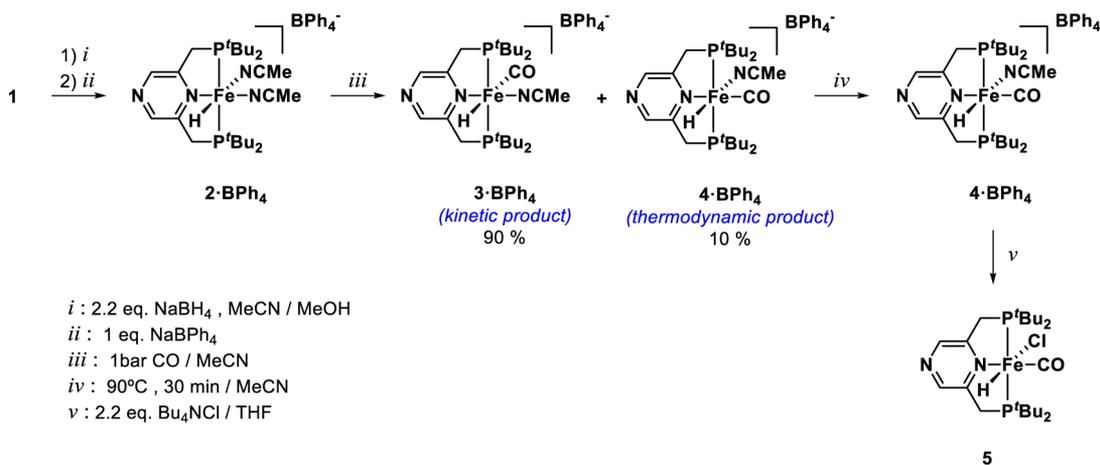
if 1 equiv of NaBPh₄ is added to the reaction mixture, counteranion exchange with NaBPh₄ yields a more stable compound **2·BPh₄**, [Fe(H)(MeCN)₂(tBu-PNzP)][BPh₄]. NMR data of **2·BPh₄** is identical to that of **2·X** (X = Br, BH₄) (with the exception of the signals for the aromatic protons of BPh₄). However, elemental analysis suggests that in the solid state the complex is better formulated as [Fe(H)-(MeCN)(tBu-PNzP)][BPh₄], in which one acetonitrile ligand has been lost. Therefore, the instability of **2·X/2·BPh₄** in organic solvents other than acetonitrile is probably due to the ease of dissociation of one of the MeCN ligands, leading to a more reactive species. The analogous complex bearing the tBu-PNP ligand shows greater stability compared to **2·BPh₄**, with similar NMR values in CD₃CN solutions.[8c] According to reactivity studies (see below) we believe that the nitrogen atom at position 4 is very likely involved in the displacement of one of the MeCN ligands in a second molecule, possibly the MeCN ligand trans to the hydride (due to hydride trans effect), when **2·BPh₄** is exposed to vacuum, leading to an oligomer (**A**) in which the hydride and MeCN are likely cis to each other.[19] Unfortunately we were not able to obtain suitable crystals for X-ray diffraction studies.

Treatment of **2·BPh₄** with carbon monoxide in acetonitrile results in a color change from deep blue to yellow within 3 h. Two isomers **3·BPh₄** and **4·BPh₄** are formed in a 9:1 ratio, respectively, according to the NMR data (Scheme 3). **3·BPh₄** can be completely transformed into **4·BPh₄** by heating this reaction mixture in acetonitrile. The appearance of a strong adsorption band at 1948 cm⁻¹ in the IR spectrum supports the formation of an iron carbonyl complex. Compound **3·BPh₄**

exhibits in the ³¹P{¹H} NMR spectrum a singlet at 109 ppm, very similar to that of its precursor, **2·BPh₄**. However, a dramatic downfield shift (ca. 13 ppm) of the hydride signal is observed (0.88 ppm, ²J_{HP} = 53 Hz). Thus, **3·BPh₄** is best described as trans-[Fe(H)(CO)(MeCN)(tBu-PNzP)], with a CO ligand located trans to the hydride. Complex **3·BPh₄** isomerizes with time to yield the thermodynamically more stable cis-[Fe(H)(CO)(MeCN)(tBu-PNzP)], **4·BPh₄**. Complete isomerization can be obtained upon heating complex **3·BPh₄** for 30 min at 90 °C in acetonitrile (Scheme 3). The CO stretching frequency for this new species appears at 1918 cm⁻¹. The phosphorus atoms resonate in the ³¹P{¹H} NMR spectrum at 113 ppm, whereas a significant change is observed for the hydride resonance in the ¹H NMR spectrum, now appearing at −17 ppm (²J_{HP} = 53 Hz).

The molecular structure of this new iron hydride species has been ascertained by X-ray diffraction studies using crystals grown by slow diffusion of diethyl ether to concentrated solutions of **4·BPh₄** in acetonitrile (Figure 3). **4·BPh₄** exhibits a distorted octahedral coordination of the iron atoms, with the cis angles in the range 82.18(4)−100.78(5)°. The Fe1−P1 and Fe1−P2 distances are 2.244(5) and 2.247(6) Å, respectively. The Fe1−N1 bond length is shorter than that observed for complex **1**, 2.011(1) Å, owing to the positively charged Fe(II) center. The Fe1−N3 distance, 1.977(2) Å, is in the expected range for Fe(II)−NCMe complexes as well as the distance for Fe−CO and Fe1−C25, 1.736(2) Å, and the iron hydride bond, Fe1−H1, 1.42(2) Å.[9c]

Addition of [Bu₄N][Cl] to a suspension of **4·BPh₄** in THF and subsequent application of vacuum results in displacement
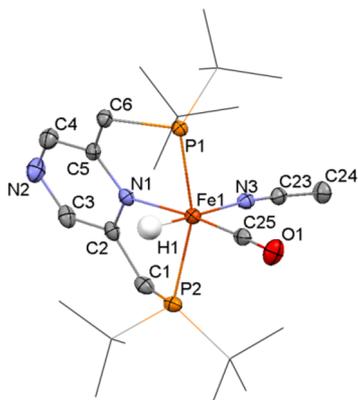
Figure 3. X-ray structure of complex **4·BPh₄**; thermal ellipsoids set at 50% probability. The counteranion is not shown and the *tert*-butyl groups are presented as wireframe for clarity. Selected bond lengths (Angstroms) and angles (degrees): Fe1−H1 1.49(2), Fe1−N1 2.011(1), Fe1−P1 2.244(5), Fe1−P2 2.245(6), Fe1−C25 1.736(2), O1−C25 1.165(2), Fe1−N3 1.977(2), N3−C23 1.140(2), C23−C24 1.462(3), N1−C2 1.354(2), N1−C5 1.350(2), N2−C3 1.327(3), N2−C4 1.337(3), C2−C3 1.391(3), C4−C5 1.389(3), P1−Fe1−P2 159.97(2), H1−Fe1−N3 176.1(8), N1−Fe1−C25 171.46(7), N1−Fe1−H1 86.2(8), H1−Fe1−C25 85.5(8), N3−Fe1−C25 98.22(7).

of the acetonitrile ligand by a chloride with concomitant precipitation of [Bu₄N][BPh₄] to give the neutral iron complex [Fe(H)(Cl)(CO)(tBu-PNzP)] **5** (Scheme 3). The cis geometry of the CO and hydride ligands is preserved according to the high-field resonance of the hydride (−20.71 ppm, $^2J_{HP}$ = 56 Hz); as expected, the preferred coordination of the hydride ligand is trans to the weaker sigma donor chloride. The lower stretching frequency of the CO ligand in the IR spectrum is in agreement with more backbonding in the neutral species. Compound **5** exhibits a singlet resonance in the $^{31}P\{^1H\}$ NMR spectrum at δ = 115 ppm. Elemental analysis is in line with the chemical structure proposed for complex **5** shown in Scheme 3.

Deprotonation of 5. Complex **5** is a suitable complex for studying the possibility of metal−ligand cooperation (MLC) by aromatization−dearomatization, since treatment with a base is expected to lead to deprotonation and dearomatization of the ligand.[9]

Treating complex **5** with 1.1 equiv of ᵗBuOK results in conversion of the orange clear solution to a brown suspension (in THF or C₆H₆), from which a brown solid was isolated by solvent removal. We presume that the brown solid, **B**, consists of aggregates, formed by coordination of the N atom at position 4 of the pyrazine ring to the deprotonated, coordinatively unsaturated iron center of another complex (Scheme 4).[20] Neutral 16-electron, five-coordinated iron(II) complexes bearing a hydride and CO ligands are rather unstable species,[8d] and the only exception reported recently is more likely formulated as an 18-electron, five-coordinated Fe(II)

complex.[6b−f,7] The amido ligand being a 4e donor in these cases and the N−Fe bond is always represented as a double bond.

Aggregation of the dearomatized units would give 18-electron, six-coordinated iron(II) complexes. Formation of these aggregates can explain the lack of solubility in THF or benzene, despite being a neutral species. In an attempt to prove the existence of a dearomatized pattern in compound **B**, NMR experiments were carried out in neat deuterated pyridine (Py-d^5) to prevent coordination of the N4 atom of the pyrazine. This approach allowed us to identify a new compound formulated as the Fe(II)−pyridine adduct, **6·Py-d^5** complex, [Fe(H)(Py-d^5)(CO)(tBu-PNzP)*] (Scheme 4, the asterisk denotes a dearomatized pincer ligand) on the basis of NMR data. **6·Py-d^5** exhibits an AB system in the $^{31}P\{^1H\}$ NMR, as two doublets are observed at δ = 96.5 and 104.9 ppm ($^2J_{PP}$ = 110 Hz), in accordance with a dearomatized system, in which one of the arms possesses a double bond. A similar conclusion can be drawn from the ^1H NMR spectrum, where the hydride signal, δ = −19.19 ppm, is no longer a triplet but a doublet of doublets, and the signal for the deprotonated arm is shifted down to δ = 4.08 ppm. In agreement with all of this, the two hydrogen atoms at the heterocyclic ring are not equivalent, resonating at δ = 7.96 and 7.12 ppm.

Complex **B** is soluble in EtOH, turning from a brown suspension to a dark but clear solution. This solution is NMR silent. Crystallization by slow diffusion of pentane resulted after 2 days in small black crystals suitable for X-ray diffraction studies. Interestingly, the ligand remains dearomatized. Complex **7**, [Fe(H)(CO)(N⁴-μ-(tBu-PNzP)*)]₆, is formed having a unique structure consisting of six iron centers bearing the new deprotonated pincer ligand (Scheme 5 and Figure 4).

Scheme 5. Formation of a Dearomatized Macrocycle upon Deprotonation of 5, Crystallized from an Ethanol/Pentane Solution at −40 °C
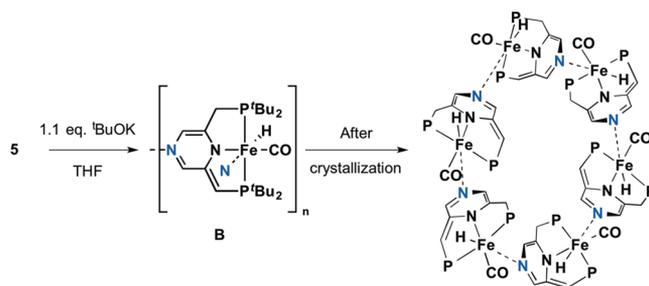
In addition to one CO and one hydride ligand, the coordination sphere around the iron atom is completed by coordination of a nitrogen atom at position 4 of the pyrazine fragment from a neighboring iron center. In each macrocycle there are 3 pairs of units showing the same bond length and

Scheme 4. Reaction of 5 with 1.1 Equiv of ᵗBuOK Gives Aggregates That Can Be Broken by Addition of Pyridine
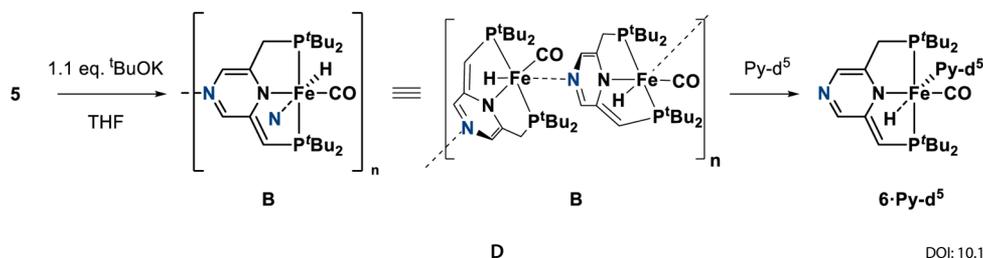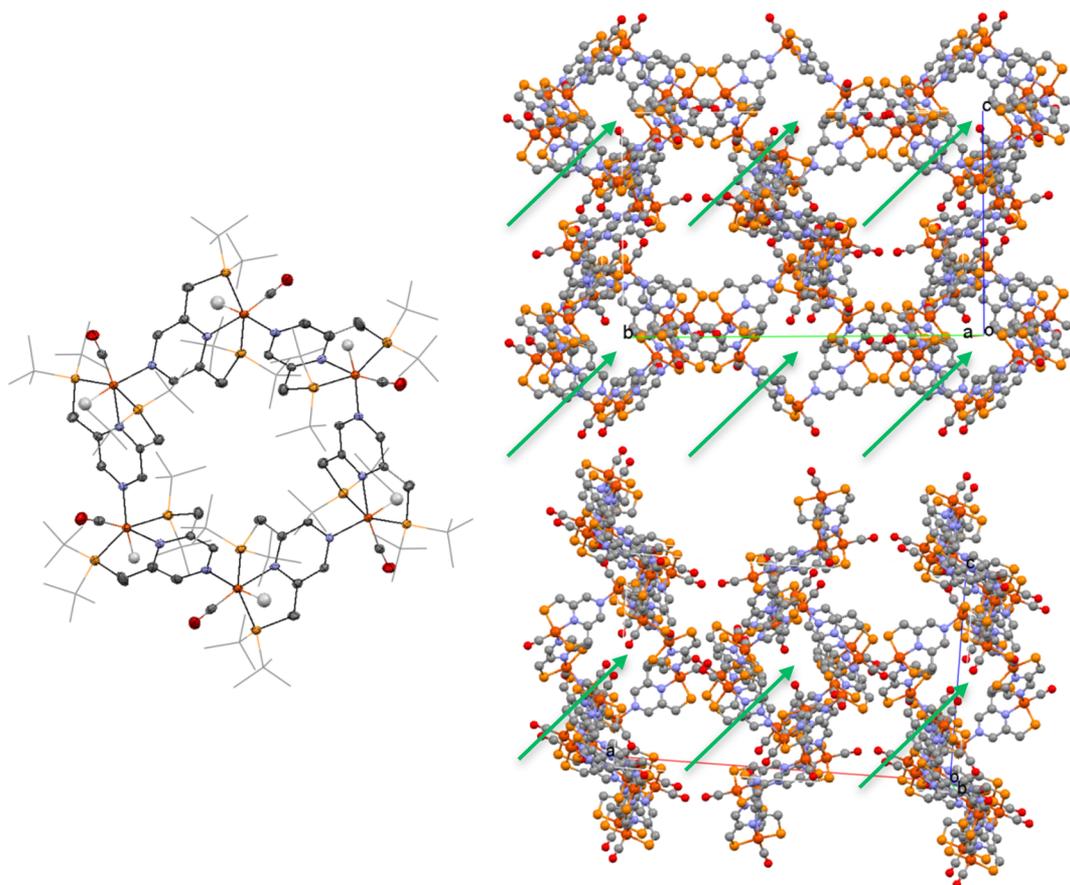
Figure 4. (Left) Molecular structure of complex **7** by X-ray crystallography; thermal ellipsoids are set at 50% probability, and the *tert*-butyl groups are presented as wireframe. The bonding of the tBu-PNzP is colored black for clarity. (Right) Ball and stick presentation of the packing of complex **7** in the unit cell in two different dispositions.

angle, and the difference between them is minimal. The unit cell is quite porous as can be seen in Figure 4. Each unit cell contains 14 macrocycle complexes, which interestingly form channels within them. The black crystals from complex **7** can be dissolved in benzene; however, within minutes the coloration changes from dark to orange and creates with time the usual brown suspension containing **B**.

Focusing merely on one of the 3 pairs (Figure 5), the geometry around the Fe(II) center is distorted octahedral, with the cis angles ranging from 82.00(8)° to 103.00(8)°. Both Fe–P distances are different, with values of 2.272(1) Å for the one attached to the deprotonated arm and 2.243(1) Å for the other one. As expected, Fe3–N5 (2.005(3) Å) is considerably shorter than Fe3–N2 (2.083(3) Å). All units present a clear dearomatized pattern. Thus, C47–C48, C49–N6, and C50–C51 bond lengths (1.379(5), 1.329(4), and 1.388(4) Å, respectively) represent double bonds, and C51–C52 (1.496(4) Å) is clearly a single bond. The Fe–CO bond separation, Fe3–C69 (1.720(4) Å), is slightly shorter than in compound **4·BPh₄**, presumably due to the higher electron density of the iron center in the neutral species, resulting in higher back-bonding.

Deprotonation of 5 Followed by Reaction with CO₂. Treatment of **5** with 1 equiv of base leads to the formation of aggregates **B**. Assuming that these aggregates are a masked coordinatively unsaturated dearomatized complex, its reactivity toward CO_2 was tested. In THF-d^8, under 1 bar of CO_2, the reaction proceeds smoothly, and after 6 h a new product forms,

which appears to be *trans*-[Fe(PNzPtBu–COO)(H)(CO)], **8**, according to NMR data. The reaction likely proceeds via a [1,3]-addition of the CO_2 molecule to the exocyclic methine carbon of the deprotonated arm of the pincer ligand and the iron metal center to produce a C–C and a Fe–O bond (Scheme 6), as previously reported for dearomatized ruthenium and rhenium complexes.[21] NMR spectroscopic data are similar to those of the previously reported complexes, particularly the complex *trans*-[Ru(PNPtBu–COO)(H)(CO)].[21a] The $^{31}P\{^1H\}$ NMR resonances of the new AB system of **8** appear at higher frequencies with respect to the pyridine adduct **6·Py-d^5** suggesting the rearomatization of the PNzP ligand in **8**.[21c] Two doublets are observed in the spectrum (THF-d^8, 25 °C) at 147.8 and 138.4 ppm with a coupling constant of $^2J_{PP} = 128$ Hz, suggesting two phosphorus nuclei in different chemical environments. The characteristic resonance for the carboxylate carbon nucleus Fe–OC(R)=O appears in the $^{13}C\{^1H\}$ NMR at 170.8 ppm and resonates as a doublet ($^2J_{CP} = 9$ Hz, THF-d^8, 25 °C). The signal of the hydride resonates as a doublet of doublets ($^2J_{HP} = 65$ Hz and $^2J_{HP} = 55$ Hz, C_6D_6, 25 °C) at −22.45 ppm. Complex **8** is highly unstable. Under CO_2 atmosphere decomposition is observed after 18 h in a J. Young NMR tube. In the absence of CO_2, complete decomposition occurs within seconds, and therefore, its characterization was only possible by NMR spectroscopy under CO_2 atmosphere.

Though complex **8** decomposes in the absence of CO_2, it is long lived enough to undergo further reactivity. In fact, when **8**
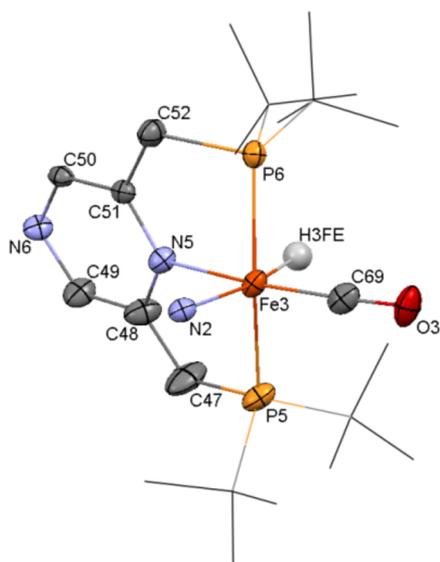
Figure 5. Molecular structure of a unit of complex **7** by X-ray crystallography; thermal ellipsoids are set at 50% probability, and *tert*-butyl groups are presents as wireframe for clarity. Selected bond lengths (Angstroms) and angles (degrees): Fe3–H3FE 1.51(3), Fe3–N5 2.005(3), Fe3–P5 2.272(1), Fe3–P6 2.243(1), Fe3–C69 1.720(4), O1–C69 1.175(4), Fe3–N2 2.083(3), N6–C49 1.329(4), N6–C50 1.370(4), N5–C48 1.388(4), N5–C51 1.353(2), C48–C49 1.423(5), C50–C51 1.388(4), C51–C52 1.496(4), C48–C47 1.379(5), P5–Fe3–P6 155.66(4), H3FE–Fe3–N5 82(1), H3FE–Fe3–N2 172(1), H3FE–Fe3–C69 88(1), N2–Fe3–C69 99.3(1), N5–Fe3–C69 169.1(1).

is exposed to 1 bar of H_2 at room temperature, a mixture of two new iron compounds is formed within minutes, together with some minor unidentified species. These new species have been identified by NMR spectroscopy as *trans*-[Fe(H)$_2$(CO)(tBu-PNzP)], complex **9**, and *trans*-[Fe(H)(OOCH)(CO)(tBu-PNzP)], complex **10** (Scheme 7 and Figure 6). Complex **9** is very likely formed through a mechanism that involves initial extrusion of a molecule of CO_2, regenerating **B**, followed by reaction with H_2 by a MLC mechanism leading to the dihydride **9**. Then, the released CO_2 can undergo an insertion process into one of the Fe–H moieties leading to complex **10**. These reactions have been performed separately starting from the dearomatized species **B** (see below).

Deprotonation of 5 and Reaction with H_2. When a mixture of **5** and 1 equiv of ^tBuOK in C_6D_6 is treated with H_2 (1 bar) a red clear solution is formed after 6 h. NMR studies indicate the formation of the trans dihydride complex **9**, [Fe(H)$_2$(CO)(tBu-PNzP)]. **9** exhibits a singlet resonance in the $^{31}P\{^1H\}$ NMR at $\delta = 137$ ppm. ^1H NMR shows a high symmetry pattern, where the hydride signal, integrating for 2 H atoms, appears at −7.03 ppm ($^1J_{HP} = 38$ Hz, notice that the coupling constant has

Scheme 7. Exposure of a Solution of Complex 8 to Hydrogen Atmosphere at Room Temperature
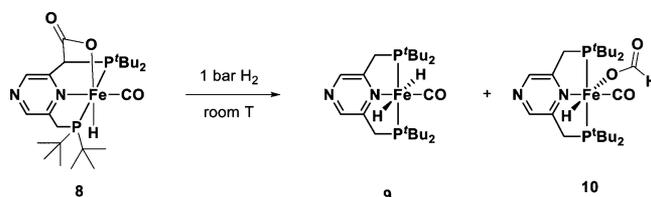
diminished by 20 Hz, compared to the related Fe(II) hydride complexes). The hydrogen atoms of the heterocycle are symmetric as expected for a nondearomatized system.

The behavior of complex **9** is rather different in protic and nonprotic solvents. When dissolved in protic solvents, such as EtOH, in a J. Young NMR tube and degassed by 3 freeze–pump–thaw cycles, the color of the solution turns from clear red to dark. Upon layering the dark solution with pentane and leaving it at −40 °C, crystals of complex **7** are obtained. Pressurization of the dark solution mentioned above with H_2 gas (1 bar) yields back complex **9**. This is a facile and clean reversible process, which occurs at room temperature, with no observed formation of free ligand or decomposition products at short periods of time. However, keeping complex **9** under 1 bar of H_2 in EtOH for 12 h results in decomposition to form the free ligand and compound **11** (Scheme 8). Complex **11** has been characterized by NMR spectroscopy as the Fe(0) complex [Fe(CO)$_2$(tBu-PNzP)].[22] Complete decomposition takes place after 36 h, generating a 1:1 mixture of the free ligand and complex **11** (Scheme 8).

On the other hand, when a solution of **9** in nonprotic solvents, such as benzene, is subjected to vacuum the signals in the ^1H NMR spectrum become broader yet complex **7** is not detected. Refilling the atmosphere of the NMR tube with H_2 does not sharpen the signals in the ^1H NMR spectrum. Complex **9** is partially stable in the solid state and in nonprotic solution, but after standing for a few days in benzene, **9** also decomposes to give free ligand and the Fe(0) complex **11**. When trying to obtain suitable crystals of **9** for X-ray diffraction studies by slow diffusion of pentane into a concentrated benzene solution of **9** at room temperature, black crystals were obtained. Interestingly, these black crystals do not belong to **9** but to the new Fe(0) complex [Fe(CO)(N^4-μ-(tBu-PNzP))]$_6$, **12**, which consists of a new 6-membered macrocomplex composed of six Fe(0) centers linked one to another through the N at position 4 of the pyrazine backbone, the CO ligand remaining bonded to the metal center (Figure 7). No dearomatized pattern is observed in the structure, as judged from the bond distances C61–C62 (1.498(4) Å) and C65–C66 (1.504(9) Å) being essentially equal.[23] Thus, complex **9** loses H_2 in ethanol solution to form the dearomatized Fe(II)

Scheme 6. Reaction of the Iron Pincer Aggregates with CO_2.
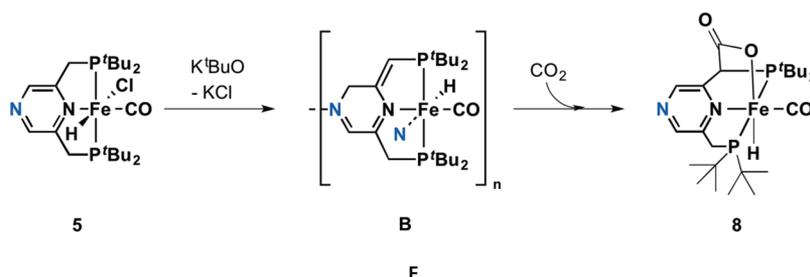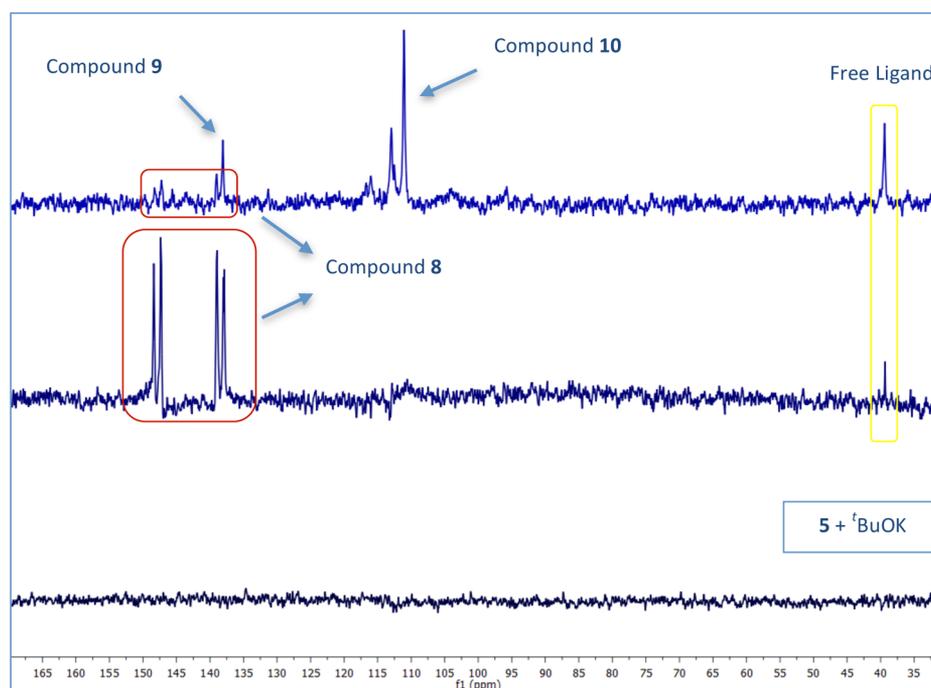
Figure 6. $^{31}P\{^1H\}$ NMR spectra of complex **5** with 1 equiv of ^tBuOK in C_6D_6 in a J. Young NMR tube (bottom), addition of 1 bar of CO_2 (middle), and addition of H_2 to previous mixture (top).

Scheme 8. Formation of Complex 9 and Its Reactivity in the Presence of H_2 or CO_2
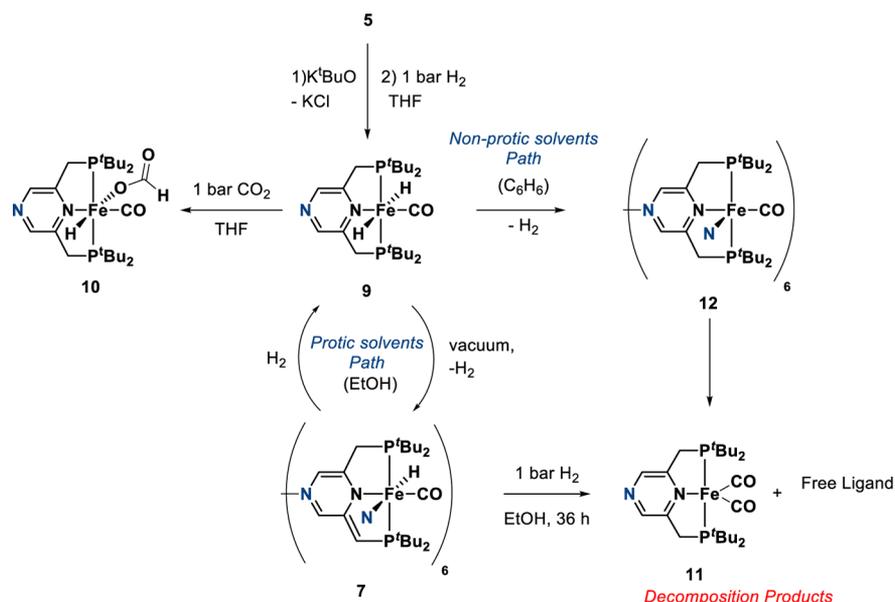
hexamer **7**, while in benzene it dehydrogenates to form the aromatic Fe(0) hexamer **12** (Scheme 8). The reason for that is not clear.

In each macrocycle there are 3 pairs of units showing the same bond lengths and angles, and the difference between them is minimal. Focusing merely on one of the 3 pairs, the iron center structure reveals a distorted square pyramid geometry around the metal, with the N atom of position 4 of the pyrazine backbone from another unit located at the apical position. The P6−Fe3−P5 and N5−Fe3−C83A angle values are 155.9(2)° and 160.0(1)°, respectively. The angles between the apical N2 atom and the surrounding atoms are almost 100° in all cases. Both Fe−P distances have similar values (2.275(1) and

2.238(1) Å). The Fe−N bond distances are not equal, being Fe3−N5 1.962(2) Å and Fe3−N2 2.043(3) Å, in contrast with complex **7**, where the Fe−N was more similar (N5 is from the PNzP ligand and N2 comes from bridging with another PNzP ligand, through the N atom in position 4).

Complex **12** appears to be an intermediate in the decomposition path from complex **9** to **11**. No dearomatized complex was detected during this crystallization.[22] We believe that extrusion of H_2 from **9** can follow several pathways, in which one of them yields the dearomatized species involving MLC with the benzylic arm of the ligand while other routes lead to decomposition products.
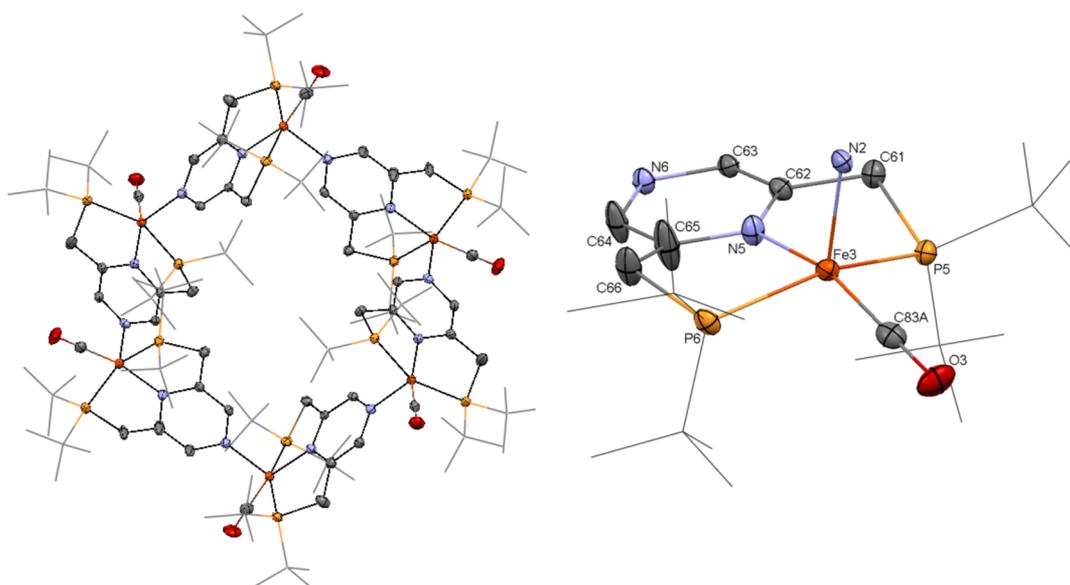
Figure 7. (Left) Molecular structure of complex **12** by X-ray crystallography; thermal ellipsoids are at 50% probability level, and the *tert*-butyl groups are presented as wireframe. The bonding of the tBu-PNzP is colored black for clarity. Benzene and pentane that cocrystallize were deleted for clarity. (Right) Molecular structure of complex **12** by X-ray crystallography; thermal ellipsoids are at 50% probability level, and the *tert*-butyl groups are presented as wireframe for clarify. Selected bond lengths (Angstroms) and angles (degrees): Fe3−N5 1.962(2), Fe3−P5 2.238(1), Fe1−P6 2.275(1), Fe1−C83A 1.726(3), O1−C83A 1.179(4), Fe3−N2 2.043(3), N6−C63 1.370(4), N6−C64 1.351(5), N5−C62 1.391(5), N5−C65 1.393(5), C62−C63 1.366(4), C64−C65 1.375(4), C61−C62 1.498(4), C65−C66 1.504(9), P5−Fe3−P6 155.92(4), N5−Fe3−N2 99.1(1), N5−Fe3−C83A 160.0(1), N2−Fe3−C69 100.9(1).
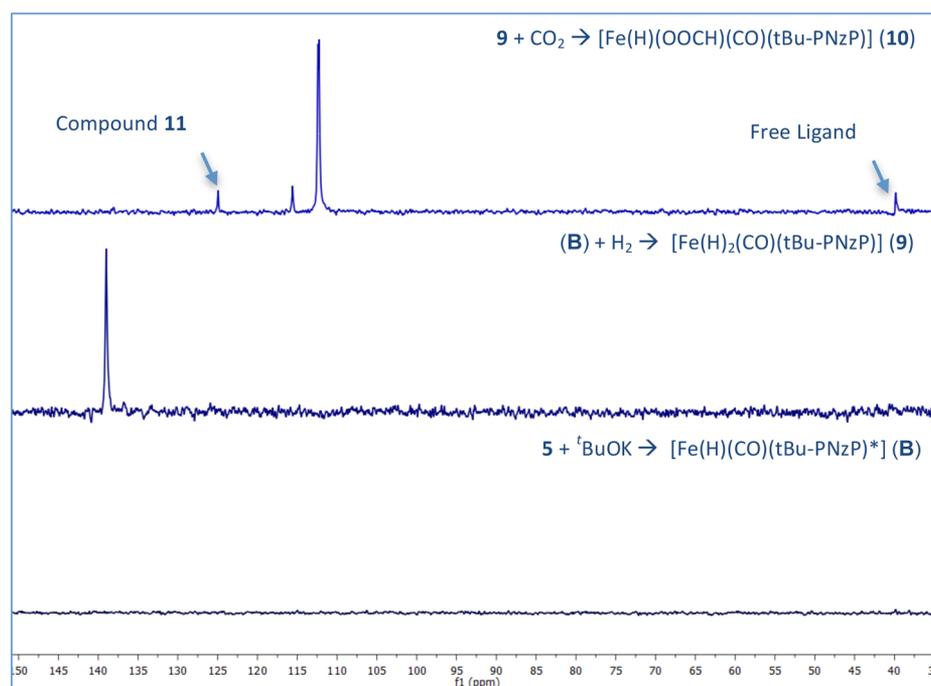
Figure 8. $^{31}P\{^1H\}$ NMR spectra of complex **5** treated with 1 equiv of ^tBuOK in C_6D_6 in a J. Young NMR tube (down), addition of 1 bar of H_2 (middle), and addition of CO_2 to previous mixture (top).

Furthermore, when complex **9** is exposed to CO_2 (1 bar) a fast reaction takes place forming the formate complex **10** in seconds (Scheme 8, Figure 8). Complex **10** exhibits a singlet resonance in the $^{31}P\{^1H\}$ NMR at δ = 112 ppm. A less symmetric environment is clearly observed in the ^1H NMR spectrum due to the coordination of the formate trans to the hydride, which now integrates for 1 H, resonating at −22.85 ppm ($^1J_{HP}$ = 55 Hz). The CH_2 groups of the PNzP ligand are diastereotopic, and a new singlet appears at 8.78 ppm, assigned to the hydrogen atom of the formate.[8c,21c] Complex **10** is not stable, decomposing after 24 h in solution to the free ligand and complex **11**. Additionally, when **10** is subjected to vacuum, CO_2 extrusion takes place and complex **9** is reformed, although this process is not clean.

Catalytic Hydrogenation of NaHCO₃. All complexes described in Scheme 3 were investigated as possible catalysts

for the hydrogenation of sodium bicarbonate. Only complex **5** showed significant catalytic activity to form sodium formate under various reaction conditions. Significant turnover numbers were obtained when water was used as solvent, with small amounts of THF as cosolvent (Table 1). With acetonitrile as

Table 1. Hydrogenation of NaHCO₃ Catalyzed by the Iron Complex 5

$$HCO_3Na + H_2 \xrightarrow[\text{H}_2\text{O/THF (10:1)}]{0.1 \text{ mol\% } \mathbf{5}} HCO_2Na + H_2O$$

entry	$p(H_2)$ [bar][b]	T [°C]	TON[c]
1	6.5	room temp	78
2	6.5	45	149
3	7	65	148
4	10	55	110
5	10	75	144
6	10	80	63
7	10	room temp	

[a]Reaction conditions: **5** (0.005 mmol), tBuOK (0.006 mmol), HCO₃Na (5 mmol), H₂O (5 mL), THF (0.5 mL), 16 h. [b]Pressure at room temperature. [c]On the basis of ¹H NMR analysis using dimethylformamide as internal standard; moles of sodium formate per mole of catalyst.

solvent no catalytic activity was observed. This is in line with the inactivity of the acetonitrile complex **4·BPh₄** in THF or H₂O/THF, possibly as a result of the strong coordination of acetonitrile. Experiments at different temperatures and pressures were conducted with 0.1 mol % of **5** in a mixture of THF:H₂O (1:10). The highest activities for complex **5** in the hydrogenation of sodium bicarbonate were observed at 45 and 65 °C at 6.5 bar of H₂ (entries 2 and 3, TON = 149 and 148, respectively), and the activity did not increase at higher pressure and temperature (entry 5, 10 bar of H₂ at 75 °C, TON = 144). For entries 2 and 3, when the reaction was run for longer periods (36 h), the TON did not increase, indicating that the maximum achievable TONs are those shown in Table 1, entries 2 and 3. Surprisingly, upon temperature increase to 85 °C, a lower TON of 63 was obtained, possibly as a result of catalyst thermal instability (entry 6). On the other hand, at room temperature (at 10 bar of H₂) no catalytic activity was observed, as reported also in other cases.[8c] Next, we studied the catalytic hydrogenation of CO₂. To this aim, mixtures of CO₂/ H₂ in a 1:2 ratio (this was the best ratio reported in the case of [Fe(H)₂(CO)(tBu-PNP)])[8c] were used in aqueous sodium hydroxide solution, instead of sodium bicarbonate, under a total pressure of 10 bar. All experiments were carried out at 55 °C while varying the concentration of sodium hydroxide in water. Sodium formate was formed with similar turnover number values as in the bicarbonate hydrogenation, when the concentration of NaOH in water was 1 M (entry 1, TON = 157). It was encouraging to observe that the turnover numbers doubled when the concentration of NaOH was raised to 2 M (entry 2, TON = 339). Further increase of NaOH concentration resulted in a moderate rise of the TON (entry 3, TON = 388), probably due to the higher concentration of carbonate dissolved in solution. With 4 M NaOH the catalyst is still active but the TON obtained is lower (entry 4, TON = 280). Entry 5 in Table 2 shows that the reaction occurs also in the absence of water, using just THF as a solvent. Sodium ethoxide was chosen to facilitate the solubility of the base compared to sodium hydroxide; however, its low solubility can

Table 2. Hydrogenation of CO₂ Catalyzed by 5

$$CO_2 + H_2 + NaOH \xrightarrow[\text{H}_2\text{O/THF (10:1)}]{0.1 \text{ mol\% } \mathbf{5}} HCO_2Na + H_2O$$

entry	$p(H_2)$ [bar][b]	$p(CO_2)$ [bar][b]	C_{NaOH} [M]	TON[c]
1	6.3	3.3	1	157
2	6.3	3.3	2	339
3	6.3	3.3	3	388
4	6.3	3.3	4	280
5[d]	6.3	3.3	1	80

[a]Reaction conditions: **5** (0.005 mmol), NaOH, H₂O (5 mL), THF (0.5 mL), 16 h. [b]Pressure at room temperature. [c]On the basis of ¹H NMR analysis using dimethylformamide as internal standard; moles of sodium formate per mole of catalyst. [d]1 M NaOEt was used in THF in the absence of water.

be reflected in the low TON obtained compared with entry 1. Furthermore, complex **9** was used to catalyze the hydrogenation of CO₂ at 80 °C, obtaining low TON values (TON = 80, entry 5, Table 2), possibly due to the thermal instability of the catalyst.

Mechanism and Conclusion. Taking into consideration the results described in the previous sections we believe that MLC is likely involved in the mechanism of the catalytic process. The first step of the hydrogenation of carbon dioxide is probably deprotonation of one of the arms of the new pincer ligand, which leads to a stable compound with a dearomatized pattern. The structure and properties of the dearomatized compound depend on the solvent. In nonprotic solvents deprotonation leads to the formation of insoluble aggregates of an unknown number of iron units, probably linked one to another by the nitrogen in position 4 of the backbone of the pincer ligand. However, the good solubility of these species in protic solvents has led to the isolation of a 6-membered ring oligo complex, whose structure has been determined by X-ray diffraction studies. The reactivity of the dearomatized species is also highly dependent on the nature of the solvent (protic vs aprotic). The dearomatized compound reacts with CO₂ and H₂ to form compounds **8** and **9**, respectively, by MLC. Compound **8** reacts with H₂, by formal substitution of CO₂ by H₂, leading to complex **9**. The dihydride complex **9** undergoes CO₂ insertion into the hydride−iron bond yielding the iron−formate complex **10**. It is likely that **10** in the presence of a base produces the dearomatized complex that reacts again with H₂, closing the catalytic cycle (Scheme 9).

It was postulated that the hydrogenation of CO₂ catalyzed by the tBu-PNP analogue iron hydride complex in water/THF involves displacement of HCO₂Na by water, followed by water displacement by H₂.[8c] Deprotonation of the H₂ ligand leads to the iron−dihydride catalytic species. This mechanism is also possible in our case. On the other hand, in this report we additionally describe catalysis in THF in the absence of water (Table 2, entry 5).

In summary, we reported in this paper a new pincer-type ligand based on a pyrazine ring which exhibits interesting reactivity. It is shown that the nitrogen atom in position 4 of the pyrazine ligand can act as a dative ligand, expanding the scope for PNP pincer complexes into macromolecular systems by the formation of aggregates. Interesting macrocycles, both aromatic and dearomatized, were isolated. In this report we provide additional support regarding the possibility of MLC involved in the catalytic process of CO₂ hydrogenation by using iron complexes in protic or nonprotic media. Further studies on

Scheme 9. Proposed Mechanism for Hydrogenation of CO₂.
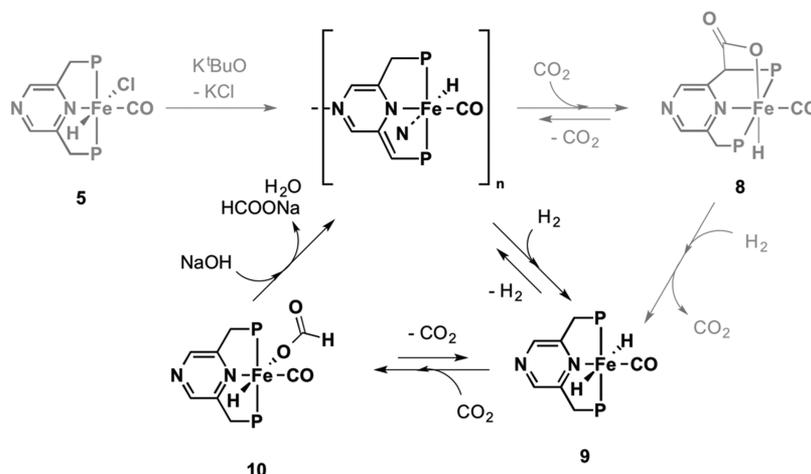
these and other systems using these pincer ligands are in progress.

■ EXPERIMENTAL SECTION

General Procedures. All experiments were carried out under an atmosphere of purified nitrogen in a Vacuum Atmospheres glovebox or using standard Schlenk techniques. All solvents were reagent grade or better. THF and *n*-pentane were refluxed over sodium/benzophenone and distilled under argon atmosphere. Ethanol, MeCN, and H_2O were cooled with liquid nitrogen and degassed under vacuum. Deuterated solvents were sparged with argon and stored in the glovebox. ^1H, ^{13}C, and ^{31}P NMR spectra were recorded using Bruker AMX-300, AMX-400, and AMX-500 NMR spectrometers. ^1H and $^{13}C\{^1H\}$ and ^{13}C-DEPTQ NMR chemical shifts are reported in ppm downfield from tetramethylsilane. ^{31}P NMR chemical shifts are reported in ppm downfield from H_3PO_4 and referenced to an external 85% solution of phosphoric acid in D_2O. NMR assignments were made based on ^1H–COSY, ^1H–^{31}P-HMQC, ^1H–^{13}C-HSQC, ^1H–^{13}C-HMBC, and ^{13}C-DEPTQ NMR spectroscopies. IR spectra were recorded on a Nicolet FT-IR spectrophotometer. Elemental analyses were performed on a Thermo Finnigan Italia S.p.A-FlashEA 1112 CHN Elemental Analyzer.

General Procedure for Catalytic Hydrogenation of HCO₃Na. A 90 mL Fischer−Porter tube was charged under nitrogen with catalyst **5** (0.005 mmol) dissolved in 0.5 mL of THF and HCO_3Na (5 mmol) dissolved in 5 mL of H_2O. The tube was pressurized at ambient temperature with hydrogen, and the solution was stirred at the specified temperature for 16 h (Table 1). After the reaction, the Fischer−Porter tube was cooled to room temperature with water and the pressure was released. Dimethylformamide (1 mmol) was added to the reaction mixture as an internal standard, and 0.05 mL of the mixture was dissolved in D_2O for determination of the yield by ^1H NMR.

General Procedure for Catalytic Hydrogenation of CO₂. A 90 mL Fischer−Porter tube was charged under nitrogen with catalyst **5** (0.005 mmol) dissolved in 0.5 mL of THF and 5 mL of an aqueous NaOH solution with the specified concentration (Table 2). The tube was pressurized with CO_2 and allowed to equilibrate for 5 min. After this period the specified hydrogen amount was added to the tube and the reaction mixture was heated to 55 °C. After the reaction, the Fischer−Porter tube was cooled with water and the pressure was released.

Dimethylformamide (1 mmol) was added to the reaction mixture as an internal standard, and 0.05 mL of the mixture was dissolved in D_2O for determination of the yield by ^1H NMR.

Ligand synthesis

tBu-PNzP. Following the report published by Neugebauer,[14] 2,6-dimethylpyrazine (5.04 g, 50 mmol), *N*-chlorosuccinimide (13.35 g,
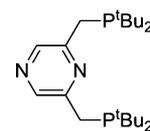
100 mmol), and dibenzoyl peroxide (0.25 g) were stirred in tetrachloromethane (100 mL) under reflux for 1 day. The solution was then cooled to 0−5 °C and filtered, washing the filtrate with tetrachloromethane (2 × 20 mL). The solvent was removed under vacuum, giving a yellow oil. The desired 2,6-bis(chloromethyl)pyrazine was separated by column chromatography [silica gel 60A, 0.040−0.063 mm, CH_2Cl_2/ethyl acetate (10:1), R_f = 0.55] in 31% yield. Later, 2,6-bis(chloromethyl)pyrazine (15 mmol) was dissolved in methanol (15 mL) followed by addition of the corresponding phosphine, R_2PH (60 mmol). This reaction mixture was heated at 45 °C for 48 h. The reaction was left to cool at room temperature, and Et_3N was added to quench the reaction (60 mmol). The solvent and other volatile compounds were removed under vacuum, and the residual solid was treated with pentane to extract the desired phosphine together with other products, leaving a red oil. The phosphine was separated by column chromatography [silica gel 60A, 0.040−0.063 mm, hexane/diethyl ether (3:1), R_f = 0.35]. tBu-PNzP, white crystalline solid, 89% yield. ^1H NMR (400 MHz, C_6D_6, 23 °C) δ: 1.05 (d, 36H, $^3J_{HP}$ = 11 Hz, $PC(CH_3)_3$), 2.88 (d, 4H, $^2J_{HP}$ = 2.4 Hz, $CH_2P^tBu_2$), 8.66 (s, 2H, pyrazine-H) ppm. $^{31}P\{^1H\}$ NMR (161 MHz, C_6D_6, 23 °C) δ: 39.4 (s) ppm. $^{13}C\{^1H\}$ NMR (100 MHz, C_6D_6, 23 °C) δ: 29.5 (d, 2C, $^2J_{CP}$ = 28 Hz, 2 $\underline{C}H_2P^tBu_2$), 29.7 (d, 12C, $^2J_{CP}$ = 28 Hz, $P[C(\underline{C}H_3)_3]_2$), 32.0 (d, 4C, 2 $P[\underline{C}(CH_3)_3]_2$), 142.6 (dd, 2C, $^2J_{CP}$ = 9 Hz, $^4J_{CP}$ = 2 Hz, pyrazine-C), 157.6 (d, 2C, $^3J_{CP}$ = 14 Hz, 2 pyrazine-C) ppm. ESI-MS (*m/z*, pos), $C_{22}H_{42}N_2P_2Na$: 419.2721 calcd, 419.2720 expt.

[Fe(Br)₂tBu-PNzP] (1). $FeBr_2$ (100 mg, 0.462 mmol) was stirred with 1.02 equiv of tBu-PNzP (184 mg, 0.462 mmol) in THF (10 mL) for 8 h, affording a red suspension. The solution was concentrated in vacuo, followed by addition of 10 mL of pentane, which led to the precipitation of an orange solid which was isolated by filtration, washed with pentane (3 × 6 mL), and dried under high vacuum. Yield: 252 mg, 89%. Single crystals were obtained from a solution of **1** in THF layered with *n*-pentane. Anal. Calcd for $C_{22}H_{42}Br_2FeN_2P_2$: C, 43.16; H, 6.92; N, 4.58. Found: C, 42.72; H, 6.94; N, 4.45.

[Fe(H)(MeCN)₂(tBu-PNzP)][BPh₄] (2·BPh₄). Complex **1** (50 mg, 0.08 mmol) was stirred in a mixture of MeOH/MeCN (4 mL, 1:1). Once the complex dissolved, 2.2 equiv of $NaBH_4$ (7 mg, 0.18 mmol) was added at once. The solution color evolved from colorless to intense dark blue, and after 15 min 1.02 equiv of $NaBPh_4$ (29 mg, 0.08 mmol) was added. Thirty minutes later the solution was layered with 15 mL of Et_2O, forming a white precipitate of NaBr and $NaBH_4$ after complete solvent mixing, and was filtered off. The filtrate was evaporated under vacuum, and the residue was dissolved in MeCN.

Layering this solution with Et_2O resulted in blue plates after 2 days. Yield: 56 mg (76%). Compound **2·BPh₄** was either not soluble (C_6D_6, toluene-d^8, MeOH-d^4) or not stable (acetone-d^6) in solvents other than CD_3CN. Due to an exchange of the coordinated MeCN with the deuterated solvent, the coordinated acetonitrile ligands could not be detected. ¹H NMR (400 MHz, CD_3CN, 23 °C) δ: −12.31 (t, 1H, $^2J_{HP}$ = 60 Hz, Fe–H), 1.35 (m, 18H, $PC(CH_3)_3$), 1.40 (m, 18H, $PC(CH_3)_3$), 3.22 (m, 2H, $CH_2P^tBu_2$), 3.41 (m, 2H, $CH_2P^tBu_2$), 6.83 (t, 4H, $^3J_{HH}$ = 7.1 Hz, BPh-H$_{para}$), 6.98 (t, 8H, $^3J_{HH}$ = 7.4 Hz, BPh-H$_{meta}$), 7.26 (br, 8H, BPh-H$_{ortho}$), 7.88 (s, 2H, pyrazine-H) ppm. ³¹P{¹H} NMR (161 MHz, CD_3CN, 23 °C) δ: 107 (s) ppm. ¹³C {¹H} NMR (100 MHz, CD_3CN, 23 °C) δ: 28.7 (br, 6C, 2 $PC(\underline{C}H_3)_3$), 28.9 (br, 6C, 2 $PC(\underline{C}H_3)_3$), 32.3 (br, 2C, 2 $\underline{C}H_2P^tBu_2$), 35.5 (br, 2C, 2 $P\underline{C}(CH_3)_3$), 36.6 (br, 2C, 2 $P\underline{C}(CH_3)_3$), 122.7 (s, 4C, BPh–C$_{para}$), 126.5 (br, 8C, BPh–C$_{meta}$), 136.7 (br, 8C, BPh–C$_{ortho}$), 137.1 (br, 2C, pyrazine-CH), 164.8 (q, 4C, $^1J_{PB}$ = 49 Hz, BPh–C$_{ipso}$), 162.9 (br, 2C, 2 pyrazine-C) ppm. Anal. Calcd for $C_{48}H_{66}BFeN_3OP_2$: C, 70.85; H, 8.18; N, 5.16. Found: C, 70.71; H, 8.07; N, 4.94.

trans-[Fe(H)(CO)(MeCN)(tBu-PNzP)][BPh₄] (*trans*-**3·BPh₄**). Complex **2-BPh₄** (50 mg, 0.06 mmol) was dissolved with MeCN (3 mL) in a Teflon capped tube and immersed in a bath of liquid nitrogen. The tube was evacuated on a high-vacuum line and cooled with liquid nitrogen, and 1 atm of carbon monoxide was added. The reaction was allowed to warm up to ambient temperature, and after 2 h under carbon monoxide atmosphere the color changed from blue to yellow-orange. All volatiles were removed in vacuo to give **3·BPh₄** together with small amounts of **4·BPh₄**. Yield: 46 mg (94%). ¹H NMR (400 MHz, CD_3CN, 23 °C) δ: 0.88 (t, 1H, $^2J_{HP}$ = 53 Hz, Fe–H), 1.44 (m, 18H, $PC(CH_3)_3$), 1.50 (m, 18H, $PC(CH_3)_3$), 3.48 (m, 2H, $CH_2P^tBu_2$), 3.50 (m, 2H, $CH_2P^tBu_2$), 6.83 (t, 4H, $^3J_{HH}$ = 7.1 Hz, BPh-H$_{para}$), 6.98 (t, 8H, $^3J_{HH}$ = 7.4 Hz, BPh-H$_{meta}$), 7.26 (br, 8H, BPh-H$_{ortho}$), 8.13 (s, 2H, pyrazine-H) ppm. ³¹P{¹H} NMR (161 MHz, CD_3CN, 23 °C) δ: 109 (s) ppm. ¹³C {¹H} NMR (100 MHz, CD_3CN, 23 °C) δ: 28.3 (d, 6C, $^2J_{CP}$ = 2 Hz, 2 $PC(\underline{C}H_3)_3$), 29.7 (d, 6C, $^2J_{CP}$ = 2 Hz, 2 $PC(\underline{C}H_3)_3$), 33.3 (d, 2C, $^1J_{CP}$ = 9 Hz, 2 $\underline{C}H_2P^tBu_2$), 36.0 (br, 2C, 2 $P\underline{C}(CH_3)_3$), 37 (br, 2C, 2 $P\underline{C}(CH_3)_3$), 122.7 (s, 4C, BPh–C$_{para}$), 126.6 (q, 8C, $^3J_{CB}$ = 2.8 Hz, BPh–C$_{meta}$), 136.7 (br, 8C, $^2J_{CB}$ = 2 Hz, BPh–C$_{ortho}$), 140.0 (d, 2C, $^3J_{CP}$ = 4 Hz, pyrazine-CH), 164.8 (q, 4C, $^1J_{PB}$ = 49 Hz, BPh–C$_{ipso}$), 160.0 (d, 2C, $^2J_{CP}$ = 5 Hz, 2 pyrazine-C), 217 (br, 1 C, Fe–CO) ppm. IR (KBr, disk): 1948 (ν CO). Due to its instability and tendency to form **4·BPh₄**, elemental analysis will be given for **4·BPh₄**.

cis-[Fe(H)(CO)(MeCN)(tBu-PNzP)][BPh₄] (**4·BPh₄**). Complex **3·BPh₄** (50 mg, 0.06 mmol) was dissolved in CH_3CN (2 mL) in a Teflon capped tube and heated at 90 °C for 30 min. Removal of the solvent in vacuo gave **4-BPh₄**, together with some impurities. After washing the yellow solid with pentane, pure **4·BPh₄** was obtained. Yield: 46 mg (91%). ¹H NMR (400 MHz, CD_3CN, 23 °C) δ: −17.0 (t, 1H, $^2J_{HP}$ = 53 Hz, Fe–H), 1.27 (m, 18H, $PC(CH_3)_3$), 1.44 (m, 18H, $PC(CH_3)_3$), 3.68 (m, 2H, $CH_2P^tBu_2$), 3.77 (m, 2H, $CH_2P^tBu_2$), 6.83 (t, 4H, $^3J_{HH}$ = 7.1 Hz, BPh-H$_{para}$), 6.98 (t, 8H, $^3J_{HH}$ = 7.4 Hz, BPh-H$_{meta}$), 7.26 (br, 8H, BPh-H$_{ortho}$), 8.58 (s, 2H, pyrazine-H) ppm. ³¹P{¹H} NMR (161 MHz, CD_3CN, 23 °C) δ: 113 (s) ppm. ¹³C {¹H} NMR (100 MHz, CD_3CN, 23 °C) δ: 28.7 (br, 6C, 2 $PC(\underline{C}H_3)_3$), 29.2 (br, 6C, 2 $PC(\underline{C}H_3)_3$), 33.5 (br, 2C, 2 $\underline{C}H_2P^tBu_2$), 36.5 (t, 2C, $^2J_{CP}$ = 11 Hz, 2 $P\underline{C}(CH_3)_3$), 37.4 (br, 2C, 2 $P\underline{C}(CH_3)_3$), 122.7 (s, 4C, BPh–C$_{para}$), 126.6 (q, 8C, $^3J_{CB}$ = 2.8 Hz, BPh–C$_{meta}$), 136.7 (br, 8C, $^2J_{CB}$ = 2 Hz, BPh–C$_{ortho}$), 141.5 (br, 2C, pyrazine-CH), 158.9 (br, 2C, 2 pyrazine-C), 164.8 (q, 4C, $^1J_{PB}$ = 49 Hz, BPh–C$_{ipso}$), 221.6 (t, 1C, $^2J_{CP}$ = 22 Hz, Fe–CO) ppm. IR (KBr, disk): 1918 (ν CO). Anal. Calcd for $C_{49}H_{66}BFeN_3OP_2$: C, 69.92; H, 7.90; N, 4.99. Found: C, 70.04; H, 7.72; N, 4.83.

[Fe(H)(Cl)(CO)(tBu-PNzP)] (**5**). Complex **4** (150 mg, 0.17 mmol) together with 2.2 equiv of Bu_4NCl (86 mg, 0.37 mmol) were dissolved in THF, giving a dark orange solution. After stirring for 30 min the solvent was removed under vacuum. The desired product was extracted from the crude residue with benzene. Removal of the solvent in vacuo gave pure **5**. Yield: 86 mg (98%). ¹H NMR (400 MHz, CD_3CN, 23 °C) δ: −20.7 (t, 1H, $^2J_{HP}$ = 56 Hz, Fe–H), 1.01 (m, 18H, $PC(CH_3)_3$), 1.45 (m, 18H, $PC(CH_3)_3$), 2.63 (m, 2H,

$CH_2P^tBu_2$), 3.53 (m, 2H, $CH_2P^tBu_2$), 7.97 (s, 2H, pyrazine-H) ppm. ³¹P{¹H} NMR (161 MHz, CD_3CN, 23 °C) δ: 115 (s) ppm. ¹³C {¹H} NMR (100 MHz, CD_3CN, 23 °C) δ: 29.3 (br, 6C, 2 $PC(\underline{C}H_3)_3$), 30.9 (br, 6C, 2 $PC(\underline{C}H_3)_3$), 33.9 (t, 2C, $^2J_{CP}$ = 5 Hz, 2 $\underline{C}H_2P^tBu_2$), 35.6 (br, 2C, 2 $P\underline{C}(CH_3)_3$), 37.7 (br, 2C, 2 $P\underline{C}(CH_3)_3$), 139.5 (t, 2C, $^3J_{CP}$ = 5 Hz, pyrazine-CH), 158.9 (t, 2C, $^2J_{CP}$ = 7 Hz, 2 pyrazine-C), 221.6 (t, 1C, $^2J_{CP}$ = 22 Hz, Fe–CO) ppm. IR (KBr, disk): 1896 (ν CO). Anal. Calcd for $C_{23}H_{43}ClFeN_2OP_2$: C, 53.45; H, 8.39; N, 5.42. Found: C, 53.02; H, 8.42; N, 5.25.

[Fe(H)(Py-d^5)(CO)(tBu-PNzP)*] (**6·Py-d^5**). Complex **5** (25 mg, 0.05 mmol) together with 1.2 equiv of tBuOK (7 mg, 0.10 mmol) were dissolved in THF, leading to formation of a dark red solution. After stirring for 30 min, the solvent was removed under vacuum and the residue was washed with pentane. The brown solid was dried to give complex **A**. Once dried, **A** was dissolved in neat Py-d^5, leading to the formation of complex **6·Py-d^5**. ¹H NMR (400 MHz, CD_3CN, 23 °C) δ: −19.24 (dd, 1H, $^2J_{HP}$ = 55 Hz, $^2J_{HP}$ = 60 Hz, Fe–H), 0.96 (m, 18H, $PC(CH_3)_3$), 1.25, 1.43 (d, 9H each, $^3J_{HP}$ = 11 Hz, $PC(CH_3)_3$), 3.89, 4.21 (dd, 1H each, $^2J_{HP}$ = 12 Hz, $^2J_{HH}$ = 16 Hz, $CH_2P^tBu_2$), 5.19 (s, 1H, CHP^tBu_2), 7.08, 7.92 (s, 1H each, pyrazine-H) ppm. ³¹P{¹H} NMR (161 MHz, CD_3CN, 23 °C) δ: 96.5, 104.9 (d, 1P each, $^2J_{PP}$ = 110 Hz) ppm. ¹³C {¹H} NMR (100 MHz, CD_3CN, 23 °C) δ: 28.5, 29.5, 30.4, 31.4 (br, 3C, $C(\underline{C}H_3)_3$), 37.4, 36.8, 37.1 (br, 1C each, $PC(\underline{C}H_3)_3$), 38.4 (d, 1C, $^2J_{CP}$ = 9 Hz, $\underline{C}H_2P^tBu_2$), 37.6 (d, 1C, $^2J_{CP}$ = 20 Hz, $\underline{C}H_2PC(CH_3)_3$), 69.3 (d, 1C, $^2J_{CP}$ = 40 Hz, $\underline{C}H$-PC($CH_3)_3$), 116.6 (m, 1C, pyrazine-CH), 117.6 (d, 1C, $^2J_{CP}$ = 10 Hz, pyrazine-$\underline{C}H$), 138.8 (d, 1C, $^2J_{CP}$ = 16 Hz, pyrazine-CH) 153.2, 164.7 (br, 1C each, pyrazine-$\underline{C}$), 222.3 (br, 1C, Fe–CO) ppm. IR (pyridine, liquid): 1868 (ν CO). The coordination of pyridine is reversible; when **6·Py-d^5** was placed under vacuum, pyridine was partially removed, which does not allow one to obtain elemental analysis.

trans-[Fe(PNzPtBu-COO)(H)(CO)] (**8**). Complex **5** (50 mg, 0.09 mmol) together with 1.2 equiv of tBuOK (13 mg, 0.12 mmol) were dissolved in THF, leading to formation of a dark red solution. After stirring for 1 h, the solvent was removed under vacuum. The desired product was washed with pentane. The solid was dried to give compound **A**, which upon addition of THF-d^8 gave a suspension that was placed in a J. Young NMR tube. The suspension was degassed by a 3 freeze–pump–thaw cycles and filled with 1 bar of CO_2. After 6 h complete reaction occurred, leading to the formation of a brown-yellow clear solution; 99.9% yield by NMR spectroscopy. ¹H NMR (400 MHz, CD_3CN, 23 °C) δ: −22.45 (dd, 1H, $^2J_{HP}$ = 47 Hz, $^2J_{HP}$ = 57, Hz Fe–H), 0.989 (m, 18H, $PC(CH_3)_3$), 1.47, 1.59 (d, 9H, $^3J_{HP}$ = 9 Hz, $PC(CH_3)_3$), 3.41 (m, 1H, $CH_2P^tBu_2$), 3.71 (m, 1H, $CH_2P^tBu_2$), 4.61 (s, 1H, CHP^tBu_2), 8.42, 8.52 (s, 1H each, pyrazine-CH) ppm. ³¹P{¹H} NMR (161 MHz, CD_3CN, 23 °C) δ: 138.4, 147.8 (d, 1P each, $^2J_{PP}$ = 128 Hz) ppm. ¹³C {¹H} NMR (100 MHz, CD_3CN, 23 °C) δ: 29.6, 30.1, 31.0 (d, 3C each, $^2J_{CP}$ = 4 Hz, $PC(\underline{C}H_3)_3$), 30.7 (s, 3C, $PC(\underline{C}H_3)_3$), 34.5 (d, 1C, $^2J_{CP}$ = 17 Hz, $\underline{C}H_2PC(CH_3)_3$), 35.3 (d, 1C, $^2J_{CP}$ = 22 Hz, $P\underline{C}(CH_3)_3$), 36.9 (d, 1C, $^2J_{CP}$ = 7 Hz, $P\underline{C}(CH_3)_3$), 37.5 (d, 1C, $^2J_{CP}$ = 8 Hz, $P\underline{C}(CH_3)_3$), 38.7 (d, 1C, $^2J_{CP}$ = 3 Hz, $P\underline{C}(CH_3)_3$), 59.7 (s, 1C, $\underline{C}HP^tBu_2$), 138.6 (d, 1C, $^4J_{CP}$ = 9 Hz, pyrazine-CH), 139.8 (d, 1C, $^4J_{CP}$ = 7 Hz, pyrazine-CH), 158.4, 159.1 (br, 1C each, pyrazine-CH), 170.7 (d, 1C, $^3J_{CP}$ = 9 Hz, $O(O=\underline{C})$-CHPC($CH_3)_3$), 225.1 (t, 1C, $^2J_{CP}$ = 25 Hz, Fe–CO) ppm. Complex **8** in the absence of CO_2 is unstable, which does not allow one to obtain its elemental analysis nor the IR spectrum.

trans-[Fe(H)₂(CO)(tBu-PNzP^{tBu})] (**9**). Complex **5** (50 mg, 0.09 mmol) together with 1.2 equiv of tBuOK (13 mg, 0.12 mmol) were dissolved in THF, leading to formation of a dark red solution. After stirring for 1 h, the solvent was removed under vacuum and the residue was washed with pentane. The resulting solid was dried to give compound **A**, to which C_6D_6 was added to give a suspension that was placed in a J. Young NMR tube. The suspension was degassed by 3 freeze–pump–thaw cycles and filled with 1 bar of H_2. After 24 h complete reaction occurred leading to the formation of a clear red solution. This solution was filtered through Celite. Removal of the solvent by vacuum yielded complex **7**. Yield: 30 mg (68%). ¹H NMR (400 MHz, tol-d^8, 23 °C) δ: −7.07 (t, 1H, $^2J_{HP}$ = 36 Hz, Fe–H), 1.31 (m, 36H, $PC(CH_3)_3$), 2.77 (m, 4H, $CH_2P^tBu_2$), 7.72 (s, 2H, pyrazine-

H) ppm. $^{31}P\{^1H\}$ NMR (161 MHz, tol-d^8, 23 °C) δ: 137 (s) ppm. $^{13}C\{^1H\}$ NMR (100 MHz, tol-d^8, 23 °C) δ: 29.6 (br, 12C, 2 PC($\underline{C}H_3$)$_3$), 34.8 (t, 2C, $^2J_{CP}$ = 5 Hz, 2 $\underline{C}H_2P^tBu_2$), 35.6 (t, 4C, $^2J_{CP}$ = 36 Hz, 2 P$\underline{C}$(CH$_3$)$_3$), 138.6 (br, 2C, pyrazine-CH), 158.8 (br, 2C, 2 pyrazine-C), 226.1 (t, 1C, $^2J_{CP}$ = 27 Hz, Fe—CO) ppm. IR (KBr, disk): 1896 (v CO). Anal. Calcd for $C_{23}H_{44}FeN_2OP_2$: C, 57.27; H, 9.19; N, 5.81. Found: C, 55.40; H, 8.98; N, 5.45. The deviation in C value may be due to the instability of complex **9** when briefly exposed to air prior to elemental analysis

[Fe(H)(OOCH)(CO)(tBu-PNzP^{tBu})] (10). Complex **5** (50 mg, 0.09 mmol) together with 1.2 equiv of tBuOK (13 mg, 0.12 mmol) were dissolved in THF, forming a dark red solution. After stirring for 1 h, the solvent was removed under vacuum and the residue was washed with pentane. The resulting solid was dried to give compound **A**, to which C_6D_6 was added to give a suspension which was placed in a J. Young NMR tube. The suspension was degassed by 3 freeze—pump—thaw cycles and filled with 1 bar of H_2. After 24 h complete reaction occurred forming a clear red solution. Once the formation of **9** was observed by ^1H NMR, the solution was degassed by a 3 freeze—pump—thaw cycles and placed under 1 bar of CO_2. The reaction occurs within minutes to give an orange solution, containing complex **10** quantitatively by NMR spectroscopy. ^1H NMR (400 MHz, CD$_3$CN, 23 °C) δ: −22.6 (t, 1H, $^2J_{HP}$ = 55 Hz, Fe—H), 1.11 (m, 18H, PC(CH$_3$)$_3$), 1.39 (m, 18H, PC(CH$_3$)$_3$), 2.85 (m, 2H, CH$_2$P$^tBu_2$), 3.54 (m, 2H, CH$_2$P$^tBu_2$), 8.13 (s, 2H, pyrazine-H), 8.98 (s, 1H, Fe-OOCH) ppm. $^{31}P\{^1H\}$ NMR (161 MHz, CD$_3$CN, 23 °C) δ: 112 (s) ppm. $^{13}C\{^1H\}$ NMR (100 MHz, CD$_3$CN, 23 °C) δ: 28.9 (br, 6C, 2 PC($\underline{C}H_3$)$_3$), 29.7 (br, 6C, 2 PC($\underline{C}H_3$)$_3$), 33.6 (t, 2C, $^2J_{CP}$ = 5 Hz, 2 $\underline{C}H_2P^tBu_2$), 35.5 (br, 2C, 2 P$\underline{C}$(CH$_3$)$_3$), 36.6 (br, 2C, 2 P$\underline{C}$(CH$_3$)$_3$), 139.7 (br, 2C, pyrazine-CH), 159.6 (br, 2C, 2 pyrazine-C), 170.5 (br, 1C, Fe—OOCH), 222.3 (br, 1C, Fe—CO) ppm.

[Fe(CO)$_2$(tBu-PNzP)] (11). Fe(CO)$_5$ (100 mg, 0.51 mmol) and tBu-PNzP (210 mg, 0.53 mmol) were dissolved in THF (10 mL) and introduced into a 50 mL Teflon capped tube. This solution was left under static vacuum and stirred under FL8BL-B UV light light for 36 h. After this time the volatiles were removed and the black-brownish solid was washed with cold pentane (−20 °C) (3 × 3 mL). The solid was dried under vacuum to give 220 mg of the desired product; yield 84%. ^1H NMR (400 MHz, C$_6$D$_6$, 23 °C) δ: 1.26 (br, 36H, PC(C$\underline{H}_3$)$_3$), 2.55 (br, 4H, CH$_2$-P$^tBu_2$), 7.90 (br, 2H, pyrazine-H) ppm. $^{31}P\{^1H\}$ NMR (161 MHz, C$_6$D$_6$, 23 °C) δ: 126 (s) ppm. $^{13}C\{^1H\}$ NMR (100 MHz, C$_6$D$_6$, 23 °C) δ: 29.6 (s, 24C, PC($\underline{C}H_3$)$_3$), 33.4 (br, 4C, 2 CH$_2$—P$^tBu_2$), 37.7 (br, 4C, P$\underline{C}$(CH$_3$)$_3$), 225.9 (br, 2C, Fe—CO) ppm. IR (KBr, disk): 1882, 1822, (v CO). Anal. Calcd for $C_{24}H_{42}FeN_2O_2P_2$: C, 56.70; H, 8.33; N, 5.51. Found: C, 56.51; H, 8.15; N, 5.05.

ASSOCIATED CONTENT

ⓢ Supporting Information

^1H and $^{31}P\{1H\}$ NMR spectra; X-ray crystal structures of **1**, **4·BPh$_4$**, **7**, and **12**. This material is available free of charge via the Internet at http://pubs.acs.org.

AUTHOR INFORMATION

Corresponding Author

*E-mail: david.milstein@weizmann.ac.il.

Notes

The authors declare no competing financial interest.

ACKNOWLEDGMENTS

REFERENCES

(1) (a) Enthaler, S.; Junge, K.; Beller, M. *Angew. Chem.* **2008**, *120*, 3363−3367. (b) *Angew. Chem., Int. Ed.* **2008**, *47*, 3317−3321. (c) Bolm, C.; Legros, J.; Le Paih, J.; Zani, L. *Chem. Rev.* **2004**, *104*, 6217−6254. (d) Correa, A.; Mancheño, O. G.; Bolm, C. *Chem. Soc. Rev.* **2008**, *37*, 1108−1117. (e) Nakamura, E.; Yoshikai, N. *J. Org. Chem.* **2010**, *75*, 6061−6067. (g) Sun, C.-L.; Li, B.-J.; Shi, Z.-J. *Chem. Rev.* **2011**, *111*, 1293−1314. (h) Quintard, A.; Rodriguez, J. *Angew. Chem., Int. Ed.* **2014**, *53*, 4044−4055.

(2) (a) Small, B. L.; Brookhart, M. *J. Am. Chem. Soc.* **1998**, *120*, 7143−7144. (b) Small, B. L.; Brookhart, M.; Bennett, A. M. A. *J. Am. Chem. Soc.* **1998**, *120*, 4049−4050. (c) Britovsek, G. J. P.; Gibson, V. C.; Kimberley, B. S.; Maddox, P. J.; McTavish, S. J.; Solan, G. A.; White, A. J. P.; Williams, D. J. *Chem. Commun.* **1998**, 849−850.

(3) (a) Bart, S. C.; Lobkovsky, E.; Chirik, P. J. *J. Am. Chem. Soc.* **2004**, 13794−13807. (b) Bart, S. C.; Lobkovsky, E.; Bill, E.; Chirik, P. J. *J. Am. Chem. Soc.* **2005**, *128*, 5302−5303. (c) Bouwkamp, M. W.; Bowman, A. C.; Lobkovsky, E.; Chirik, P. J. *J. Am. Chem. Soc.* **2006**, *128*, 13340−13341. (d) Tondreau, A. M.; Atienza, C. C. H.; Weller, K. J.; Nye, S. A.; Lewis, K. M.; Delis, G. P.; Chirik, P. J. *Science* **2012**, *335*, 567−570. (e) Yu, R. P.; Darmon, J. M.; Hoyt, J. M.; Margulieux, G. W.; Turner, Z. R.; Chirik, P. J. *ACS Catal.* **2012**, *2*, 1760−1764.

(4) (a) Hoyt, J. M.; Sylvester, K. T.; Semproni, S. P.; Chirik, P. J. *J. Am. Chem. Soc.* **2013**, *135*, 4862−4877. (b) Milsmann, C.; Semproni, S. P.; Chirik, P. J. *J. Am. Chem. Soc.* **2014**, *136*, 12099−12107.

(5) (a) Bichler, B.; Holzhacker, C.; Stöger, B.; Puchberger, M.; Veiros, L. F.; Kirchner, K. *Organometallics* **2013**, *32*, 4114−4121. (b) Peng, D.; Zhang, Y.; Du, X.; Zhang, L.; Leng, X.; Walter, M. D.; Huang, Z. *J. Am. Chem. Soc.* **2013**, *135*, 19154−19166. (c) Zhao, H.; Sun, H.; Li, X. *Organometallics* **2014**, *33*, 3535−3539. (d) Bhattacharya, P.; Krause, J. A.; Guan, H. *J. Am. Chem. Soc.* **2014**, *136*, 11153−11161.

(6) (a) Koehne, I.; Schmeier, T. J.; Bielinski, E. A.; Pan, C. J.; Lagaditis, P. O.; Bernskoetter, W. H.; Takase, M. K.; Würtele, C.; Hazari, N.; Schneider, S. *Inorg. Chem.* **2014**, *53*, 2133−2143. (b) Alberico, E.; Sponholz, P.; Cordes, C.; Nielsen, M.; Drexler, H.-J.; Baumann, W.; Junge, H.; Beller, M. *Angew. Chem., Int. Ed.* **2013**, *52*, 14162−14166. (c) Chakraborty, S.; Dai, H.; Bhattacharya, P.; Fairweather, N. T.; Gibson, M. S.; Krause, J. A.; Guan, H. *J. Am. Chem. Soc.* **2014**, *136*, 7869−7822. (d) Werkmeister, S.; Junge, K.; Wendt, B.; Alberico, E.; Jiao, H.; Baumann, W.; Junge, H.; Gallou, F.; Beller, M. *Angew. Chem., Int. Ed.* **2014**, *53*, 8722−8726. (e) Chakraborty, S.; Brennessel, W. W.; Jones, W. D. *J. Am. Chem. Soc.* **2014**, *136*, 8564−8567. (f) Bielinski, E. A.; Lagaditis, P. O.; Zhang, Y.; Mercado, B. Q.; Würtele, C.; Bernskoetter, W. H.; Hazari, N.; Schneider, S. *J. Am. Chem. Soc.* **2014**, *136*, 10234−10237.

(7) Chakraborty, S.; Lagaditis, P. O.; Förster, M.; Bielinski, E. A.; Hazari, N.; Holthausen, M. C.; Jones, W. D.; Schneider, S. *ACS Catal.* **2014**, DOI: 10.1021/cs5009656.

(8) (a) Zhang, J.; Gandelman, M.; Shimon, L. J. W.; Rozenberg, H.; Milstein, D. *Organometallics* **2004**, *23*, 4026. (b) Langer, R.; Leitus, G.; Ben-David, Y.; Milstein, D. *Angew. Chem., Int. Ed.* **2011**, *50*, 2120−2124. (c) Langer, R.; Diskin-Posner, Y.; Leitus, G.; Shimon, L. J. W.; Ben-David, Y.; Milstein, D. *Angew. Chem., Int. Ed.* **2011**, *50*, 9948−9952. (d) Langer, R.; Iron, M. A.; Konstantinovski, L.; Diskin-Posner, Y.; Leitus, G.; Ben-David, Y.; Milstein, D. *Chem.—Eur. J.* **2012**, *18*, 7196−7209. (e) Zell, T.; Butschke, B.; Ben-David, Y.; Milstein, D. *Chem.—Eur. J.* **2013**, *19*, 8068−8072. (f) Zell, T.; Langer, R.; Iron, M. A.; Konstantinovski, L.; Shimon, L. J. W.; Diskin-Posner, Y.; Leitus, G.; Balaraman, E.; Ben-David, Y.; Milstein, D. *Inorg. Chem.* **2013**, *52*, 9636−9649. (g) Zell, T.; Milko, P.; Fillman, K. L.; Diskin-Posner, Y.; Bendikov, T.; Iron, M. A.; Leitus, G.; Ben-David, Y.; Neidig, M. L.; Milstein, D. *Chem.—Eur. J.* **2014**, *20*, 4403−4413. (h) Zell, T.; Ben-David, Y.; Milstein, D. *Angew. Chem., Int. Ed.* **2014**, *53*, 4685−4689.

(9) Reviews: (a) Gunanathan, C.; Milstein, D. *Chem. Rev.* **2014**, *114*, 12024−12087. (b) Balaraman, E.; Milstein, D. *Top. Organomet. Chem.* **2014**, *48*, 19−44. (c) Gunanathan, C.; Milstein, D. *Science* **2013**, *341*, 1229712. (d) Gunanathan, C.; Milstein, D. *Top. Organomet. Chem.* **2011**, *37*, 55−84. (e) Gunanathan, C.; Milstein, D. *Acc. Chem. Res.* **2011**, *44*, 588−602. (f) Milstein, D. *Top. Catal.* **2010**, *53*, 915−923.

(10) Liberman-Martin, A. L.; Bergman, R. G.; Don Tilley, T. *J. Am. Chem. Soc.* **2013**, *135*, 9612−9615.

(11) Weisman, A.; Gozin, M.; Kraatz, H.-B.; Milstein, D. *Inorg. Chem.* **1996**, *35*, 1792.

(12) (a) Fujihara, T.; Tani, Y.; Semba, K.; Terao, J.; Tsuji, Y. *Angew. Chem., Int. Ed.* **2012**, *51*, 11487−11490. (b) Beydoun, K.; vom Stein, T.; Klankermayer, J.; Leitner, W. *Angew. Chem., Int. Ed.* **2013**, *52*, 9554−9557. (c) Greenhalgh, M. D.; Thomas, S. P. *J. Am. Chem. Soc.* **2012**, *134*, 11900−11903. (d) Yonemoto-Kobayashi, M.; Inamoto, K.; Tanaka, Y.; Kondo, Y. *Org. Biomol. Chem.* **2013**, *11*, 3773−3775.

(13) (a) Ziebart, C.; Federsel, C.; Anbarasan, P.; Jackstell, R.; Baumann, W.; Spannenberg, A.; Beller, M. *J. Am. Chem. Soc.* **2012**, *134*, 20701−20704. (b) Jeletic, M. S.; Mock, M. T.; Appel, A. M.; Linehan, J. C. *J. Am. Chem. Soc.* **2013**, *135*, 11533−11536. (c) Filonenko, G. A.; van Putten, R.; Schulpen, E. N.; Hensen, E. J. M.; Pidko, E. A. *Chem. Catal. Chem.* **2014**, *6*, 1526−1530. (d) Burgemeister, T.; Kastner, F.; Leitner, W. *Angew. Chem.* **1993**, *105*, 781−783. (e) *Angew. Chem., Int. Ed. Engl.* **1993**, *32*, 739−741. (f) Jessop, P. G.; Ikariya, T.; Noyori, R. *Nature* **1994**, *368*, 231−233. (g) Munshi, P.; Main, A. D.; Linehan, J.; Tai, C. C.; Jessop, P. G. *J. Am. Chem. Soc.* **2002**, *124*, 7963−7971. (h) Tanaka, R.; Yamashita, M.; Nozaki, K. *J. Am. Chem. Soc.* **2009**, *31*, 14168−14169. (i) Schmeier, T. J.; Dobereiner, G. E.; Crabtree, R. H.; Hazari, N. *J. Am. Chem. Soc.* **2011**, *133*, 9274−9277. (j) Hull, J. F.; Himeda, Y.; Wang, W. H.; Hashiguchi, B.; Periana, R.; Szalda, D. J.; Meckerman, J. T.; Fujita, E. *Nat. Chem.* **2012**, *4*, 383−388. (k) Wang, W. H.; Badiei, Y. M.; Hull, J. F.; Szalda, D. J.; Meckerman, J. T.; Fujita, E. *Inorg. Chem.* **2013**, *52*, 12576−12586. (l) Boddien, A.; Gärtner, F.; Federsel, C.; Sponholz, P.; Melmann, D.; Jackstell, R.; Junge, H.; Beller, M. *Angew. Chem., Int. Ed.* **2011**, *50*, 6411−6414. (m) Federsel, C.; Boddien, A.; Jackstell, R.; Jennerjahn, R.; Dyson, P. J.; Scopellite, R.; Laurenczy, G.; Beller, M. *Angew. Chem., Int. Ed.* **2010**, *49*, 9777−9780. (n) Drake, J. L.; Manna, C. M.; Byers, J. *Organometallics* **2013**, *32*, 6891−6894. (o) Tanka, R.; Yamashita, M.; Cung, L. W.; Morokuma, K.; Nozaki, K. *Organometallics* **2011**, *30*, 6742−6750.

(14) Eiermann, U.; Krieger, C.; Neugebauer, F. A.; Staab, H. A. *Chem. Ber.* **1990**, *123*, 523−533.

(15) Hermann, D.; Gandelman, M.; Rozenberg, H.; Shimon, L. J. W.; Milstein, D. *Organometallics* **2002**, *21*, 812.

(16) Evans, D. F. *J. Chem. Soc.* **1959**, 2003.

(17) Addison, A. W.; Rao, T. N. *J. Chem. Soc., Dalton Trans.* **1984**, *7*, 1349−1356.

(18) Zhang, J.; Gandelman, M.; Herrma, D.; Leitus, G.; Shimon, L. J. W.; Ben-David, Y.; Milstein, D. *Inorg. Chim. Acta* **2006**, *359*, 1955−1960.

(19) Further, in this report it will be shown that the N atom in position 4 is able to coordinate to the metal center to form aggregates and even defined macromolecules.

(20) Examples of pyrazine acting as a bridging ligand with Ru(II): (a) Adeyemi, S. A.; Johnson, E. C.; Miller, F. J.; Meyer, T. J. *Inorg. Chem.* **1973**, *12*, 2371−2374. (b) Ferretti, A.; Lami, A. *Chem. Phys.* **1994**, *186*, 143−151. (c) Londergan, C. H.; Salsman, J. C.; Ronco, S.; Kubiak, C. P. *Inorg. Chem.* **2003**, *42*, 926−928. With Fe(II): (d) Bohm, M. C. *Chem. Phys.* **1983**, *76*, 1−14. (e) Haynes, J. S.; Sams, J. R.; Thompson, R. C. *Inorg. Chem.* **1986**, *25*, 3740−3744. (f) Haynes, J. S.; Kostikas, A.; Sams, J. R.; Simopoulos, A.; Thompson, R. C. *Inorg. Chem.* **1987**, *26*, 2630−2637. (g) Real, J. A.; De Munno, G.; Muñoz, M. C.; Julvel, M. *Inorg. Chem.* **1991**, *30*, 2701−2704.

(21) This type of CO_2 activation has been reported with Ru: (a) Vogt, M.; Gargir, M.; Iron, M. A.; Diskin-Posner, Y.; Ben-David, Y.; Milstein, D. *Chem.—Eur. J.* **2012**, *18*, 9194−9197. (b) Hu, C. A.; Kampf, J. W.; Sanford, M. S. *Organometallics* **2012**, *31*, 4643−4645. (c) With Re: Vogt, M.; Nerush, A.; Diskin-Posner, Y.; Ben-David, Y.; Milstein, D. *Chem. Sci.* **2014**, *5*, 2043−2051.

(22) Complex **11** has been synthesized independently from $Fe(CO)_5$ and tBu-PNzP, see Experimental Section.

(23) Only free ligand was detected by the ^{31}P NMR spectra of the remaining solution.